THE DERIVATION OF THE ABSORPTION MODEL
FROM FEYNMAN DIAGRAMS

Clifford Risk

January 14, 1970

LAWRENCE RADIATION LABORATORY
UNIVERSITY of CALIFORNIA BERKELEY

DISCLAIMER

CONTENTS

THE DERIVATION OF THE ABSORPTION MODEL

FROM FEYNMAN DIAGRAMS[*]

Clifford Risk

Lawrence Radiation Laboratory
University of California
Berkeley, California

January 14, 1970

Lectures given at the theory seminar summarizing work

by Frank Henyey and Clifford Risk

ABSTRACT

In these lectures I will present a summary of work[*] carried out
by Frank Henyey and I that derives the absorption model from field
theoretic diagrams. The work developed from a program being carried
out at Michigan that describes a large number of quasi-two-body reactions
with the absorption model. This model involves a Regge cut correction
to Regge pole amplitudes which is generated by the exchange of the
Regge pole and a Pomeranchuk. The cut features the product of the
Reggeon and Pomeron (without complex conjugation of either) and a large
magnitude for the cut (coherent inelastic effects add to the original
cut term).

---

[*] A final version is being prepared for publication.

The fundamental physical assumption of our derivation is that physical particles are composite objects of constituent pieces of matter. In a scattering process, some of the constituent matter takes part in the scattering while the rest stands by as a spectator. These ideas lead us to describe double scattering processes by a class of diagrams involving exchange of two Reggeons in the cross channel and propagation of composite physical particles in the direct channel. When the direct channel particles are Reggeized, we obtain an expression for the Regge box diagram.

We begin our analysis of diagrams by discussing the AFS diagram and similar diagrams to demonstrate how the absence of third double spectral functions leads to the absence of a cut. For simple diagrams, we find that we are forced to invoke properties of form factors to show absence of the cut, but that for sufficiently composite diagrams the absence of the cut rests solely on the absence of the third double spectral functions.

Next we discuss the Mandelstam diagram and similar diagrams to demonstrate how the presence of third double spectral functions leads to cuts. For each diagram we bring the expression for the amplitude to the form of the absorption model.

Finally, we study the general class of diagrams referred to above. These diagrams contain (i) compositeness in the direct channel (physical particles are composite), (ii) third double spectral functions (physical particles have definite signature), and (iii) two Reggeon

exchange (double scattering and the Glauber spectator approximation).
(iv) By assuming saturation of direct channel amplitudes by physical
states, we are led (v) to an absorption formula (no complex conjugations)
that (vi) includes the coherent inelastic factor λ (diffraction
production of direct channel resonances).

NOTE

The Sudakov variable techniques, used extensively here, were
first applied to diagrams with Reggeons in a comprehensive work to
develop a Reggeon calculus by V. N. Gribov (1967). In the present
work we have employed these techniques to analyze the diagrams
considered here in obtaining the absorption model. After our work was
completed (August, 1969), a series of six papers appeared by Gribov
and Migdal, Kaidalov and Karnakov, and ter-Martirosyan which extended
the earlier work of Gribov, and, among other things, obtained the
absorption model. In Part III we compare our approach with theirs
and discuss the similarities and differences.

1.   INTRODUCTION

The idea that the asymptotic behavior of a scattering amplitude
$A(s,t)$ is determined by singularities of the partial wave amplitude
$f_j(t)$ in the complex j plane is ten years old.[1] During this decade,
this idea has been studied both phenomenologically with various models
that describe specific reactions,[2] and theoretically with the investiga-
tion of sums of Feynman diagrams that define amplitudes with various
types of j plane singularities.[3,4]

The main school of thought has been that $f_j(t)$ is meromorphic
in the j plane with simple poles at values $j = \alpha_i(t)$ that correspond
to physical particles. Phenomenological models with these Regge poles
were used to fit a large number of elastic and quasi-two body reactions.
Meanwhile, the theoretical study of various field theories led to the
conclusion that Regge poles arise there also.

However, the use of phenomenological models with poles alone
led to several difficulties and complications in the attempting to
explain features of differential cross sections[7]-such as dips, crossovers,
and forward peaks (in π exchange reactions)-and of total cross sections-
such as the rise at Serpukhov energies. This suggested that in the
j plane the properties of $f_j(t)$ might be more involved than containing
poles only. Meanwhile, the study of field theory models produced
amplitudes with fixed poles, moving cuts, fixed cuts, and essential
singularities.

One of the earlier models with more complicated singularities
was developed by Abers[6] et al (following earlier work by Udgaonkar

and Gell-Mann[5]) in the study of π-deuteron scattering. Glauber[8,9]

had shown that the amplitude $A_{\pi d}$ could be expressed as a sum of

terms[31]

$$A_{\pi d}(s,t) = G\left(-\frac{t}{4}\right)[A_{\pi p}(s_1,t) + A_{\pi n}(s_2,t)]$$

$$+ \frac{i}{2\pi^{3/2}} \int G(p^2) A_{\pi p}\left[s_1, -\left(\frac{q}{2} + p\right)^2\right] A_{\pi n}\left[s_2, -\left(\frac{q}{2} - p\right)^2\right] d^2 p$$

$$(1)$$

where $A_{\pi p}$, $A_{\pi n}$ are single scattering terms, s_i are center-of-mass

energy squares, $t = -q^2$, p is a two-dimensional vector perpendicular

to the incident direction, and $G(p^2)$ is the deuteron form factor.

Abers et al then showed that the terms of Eq. (1) correspond to the

amplitudes for the diagrams of Fig. 1,

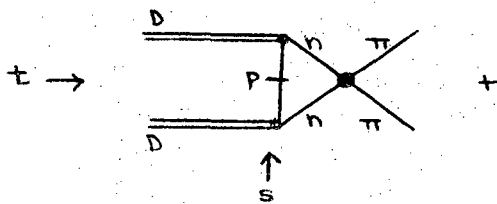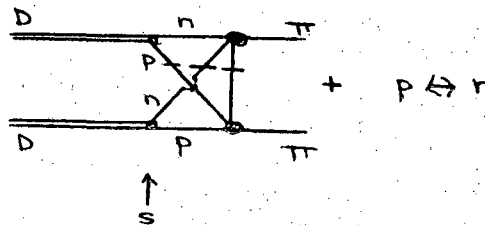Fig. 1a   Fig. 1b

where the particles in the direct channel (cut by the dashed line)

are to be evaluated near mass shell. Furthermore, if the single

scattering terms were given by Regge poles

$$A_{\pi p}(s,t) = \beta(t) s^{\alpha(t)} \qquad (2)$$

then the double scattering term of Eq. (1) took the form of an

amplitude with a cut in the j plane at $j(t) = 2\alpha(\frac{t}{4}) - 1$,

$$A(\text{double}) = \frac{s^{j(t)}}{\ln s} .$$

<div align="right">(3)</div>

This cut term, the Glauber shadow correction, was observed experimentally in differential and total cross sections. However, it was next shown that if in Fig. 1b the contribution was evaluated from the region of integration where the π was far off mass shell, this exactly cancelled the earlier cut term of Eq. (3). The sum of both contributions behaved as $1/s^3$ and had no leading cut.[30]

This type of difficulty also occurs in recent models that describe two-body processes in terms of a multiple scattering series. In describing $\pi^- p \to \pi^0 n$, one is led to the formula[32]

$$A(s,t) = A_\rho(s,t) - \frac{i}{32\pi^2} \int d\Omega\, A_\rho(s,t_1)\, A_{e\ell}(s,t_2) ,$$

<div align="right">(4)</div>

where A_ρ is the amplitude for ρ exchange, and $A_{e\ell}$ is the elastic π-nucleon amplitude. This can be derived from either a Glauber eikonal series[10,11] or from the Sopkovitch formula.[7] It can also be derived from Feynman diagrams of the type
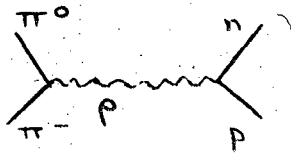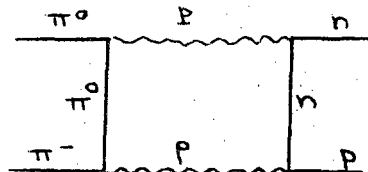
Fig. 2a   Fig. 2b

The second term in Eq. (4) corresponds to the contribution from Fig. 2b in which the direct channel π^0, n are evaluated near mass

shell. However, if one evaluates the contribution from the region

where the π^0,n go off mass shell, the previous term is again exactly

cancelled, and their sum has no cut.

The difficulty encountered in both of these examples is

related to the diagram version of the work of AFS. If one evaluates

the discontinuity of the amplitude of Fig. 3a across the branch cut

of the two particle direct channel state (Fig. 3b),
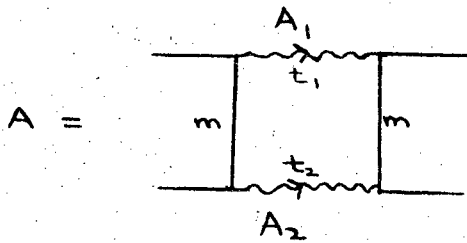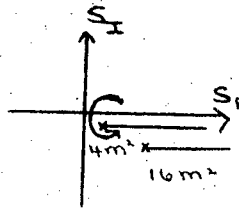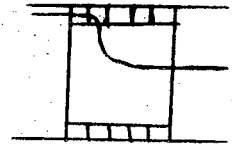
Fig. 3a   Fig. 3b   Fig. 3c

then one finds[12] that

$$\text{Im } A(s,t) \propto \int \frac{d^2 \underset{\sim}{k}}{s} A_1(s,t_1) A_2^*(s,t_2) . \tag{5}$$

Hence A(s,t) has a branch point at $j(t) = 2\alpha(t/4) - 1$. However,

it is known that a Reggeon can be represented as a sum of ladder

diagrams.[3] If these are substituted in Fig. 3a to give Fig. 3c,

and if the new contributions to the unitarity equation are added to

Eq. (5), then the cut is exactly cancelled.[13]

While the three diagrams considered do not have cuts, there

are diagrams which do have cuts, for example, the double cross

diagram[3,14] of Fig. 4.

Fig. 4

In the present work we will reconcile these results for
Feynman diagrams on the one hand with the experimentally valid
multiple scattering models on the other. To do this, we start from
assumptions about the composite structure of physical particles, and
combine this with the ideas of multiple scattering. This leads us
to a class of Feynman diagrams, which can be evaluated in the high-
energy limit. The final expression we are led to agrees with the
multiple scattering models discussed above.

The organization of the paper is as follows. In Sec. 2 we
discuss the AFS diagram; it provides the simplest example of a diagram
without a cut. In Sec. 3 we discuss the double cross diagram of
Fig. 4, the simplest example of a diagram with a cut, and bring the
expression for the amplitude to a form similar to the absorption model.
Next we extend the results to a more complicated diagram with a cut.
In Sec. 4 we discuss two further diagrams without cuts, drawing out
the role that third double spectral functions and form factors play
in the analysis of cuts. All this leads to the analysis in Sec. 5
of a very general class of diagrams, in which the presence of a cut
is thrown completely onto the presence of third double spectral
functions.

In Part II we present our view of the composite structure of physical particles and combine this with the diagram results to obtain the derivation of the absorption model.

In Part III we compare our results with the work of Gribov et al.

In Part IV we summarize the assumptions, results, and unsolved problems of the paper.

PART I. MATHEMATICAL DERIVATIONS

Two approaches have been developed in the study of asymptotic behavior of Feynman diagrams. One approach[3,15] has involved the study of diagrams with internal elementary particles only (as opposed to internal Reggeons). The amplitude is written in terms of Feynman parameters

$$A(s,t) = \int_0^1 \pi \, d\, \alpha_i \, \frac{\delta(1 - \Sigma\alpha_i)}{[D(\alpha,s,t)]^p} \, C(\alpha)^{p-2} \,, \qquad (6)$$

and the integraion is performed explicitly over the region of integration where the leading behavior in s is attained. For example, for the box diagram with spinless particles one finds

$$A(s,t) \rightarrow \frac{\ln s}{s} K(t) \qquad (7)$$

where $K(t)$ is a known function. It is then found that by summing over certain classes of diagrams, amplitudes are obtained which correspond to moving Regge poles, fixed poles, moving cuts, fixed cuts, and essential singularities.

The second approach (which we shall use) is used in studying diagrams that contain both internal Reggeons and internal elementary particles. The amplitude is written directly in terms of its internal Regge amplitudes and elementary propagators, and then certain principles are invoked to extract the asymptotic behavior and display it in a recognizable form. This approach has been developed in two forms-by Rothe[16] and Wilkin[17] (using mass variables) and by Gribov[18] (using Sudakov variables). We shall use both of these methods.

2. THE AFS DIAGRAM

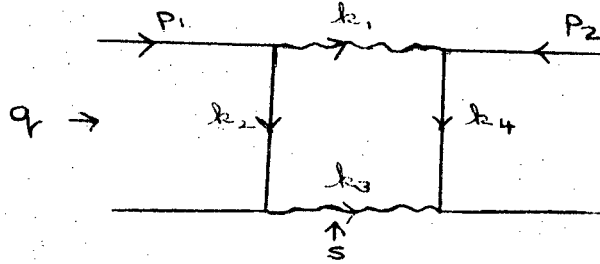To begin with we consider the AFS diagram of Fig. 5. We briefly discuss Rothe's treatment

Fig. 5

because it illustrates principles we shall need later on. The amplitude is given by

$$A(s,t) \; \varpropto \; \int d^4k_1 \; \frac{R(s,k_1^2; \; k_2^2,k_4^2) \; R(s,k_3^2; \; k_2^2,k_4^2)}{(k_2^2 - m^2 + i\epsilon)(k_4^2 - m^2 + i\epsilon)} \; . \tag{8}$$

To evaluate the asymptotic behavior of $A(s,t)$ it is convenient to introduce mass variables

$$s_1 = k_2^2, \quad s_2 = k_4^2, \quad t_1 = k_1^2, \quad t_2 = k_3^2 . \tag{9}$$

Then, in the limit of large s, Eq. (4) becomes

$$A(s,t) \; \propto \; \frac{1}{s} \int_{\lambda \le 0} \frac{dt_1 dt_2}{(-\lambda)^{\frac{1}{2}}} \int_{\lambda \ge 0} ds_1 ds_2 \; \frac{R(s,t_1; \; s_1,s_2) \; R(s,t_2; \; s_1,s_2)}{(s_1 - m^2 + i\epsilon)(s_2 - m^2 + i\epsilon)}$$

$$\tag{10}$$

where

$$\lambda(t,t_1,t_2) = t^2 + t_1^2 + t_2^2 - 2tt_1 - 2tt_2 - 2t_1 t_2 \tag{11a}$$

$$\lambda(s,s_1,s_2) = s^2 + s_1^2 + s_2^2 - 2ss_1 - 2ss_2 - 2s_1 s_2 \tag{11b}$$

and the ranges of integration are shown in Fig. 6.
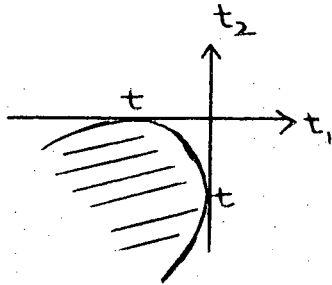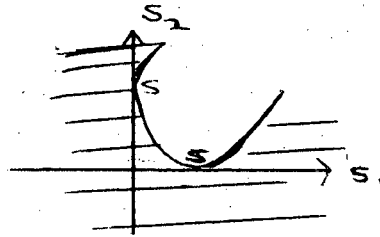
Fig. 6a   Fig. 6b

Now as a function of s_1, the integrand of Eq. (10) has singularities in the lower half plane consisting of a pole at $s_1 = m^2 - i\epsilon$ and cuts from the form factors of the Regge amplitudes. Also, it is known[14,19] that as s_1 becomes large

$$R(s,t; s_1,s_2) \rightarrow 1/s . \tag{12}$$

(This is valid in the limit s fixed, $s_1 \rightarrow \infty$ and also in the limit $s \sim s_1 \rightarrow \infty$.) The s_1 integration runs from $s_1 = -\infty$ to $s_1 \sim s$.
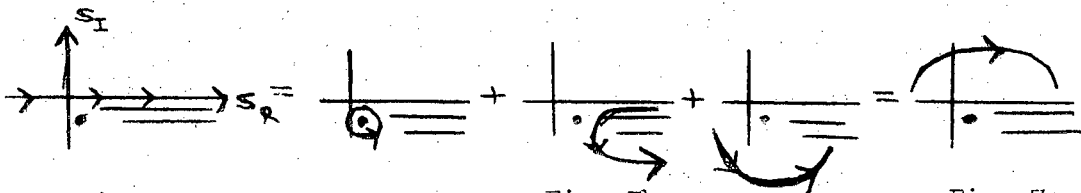

Fig. 7a   Fig. 7b   Fig. 7c

Therefore, if we distort the s_1-and similary s_2-integration in the lower half plane, we obtain

$$A(s,t) \propto \frac{1}{s} \int \frac{dt_1 dt_2}{(-\lambda)^{\frac{1}{2}}} R(s,t_1) R(s,t_2) + A_2(s,t) + A_3(s,t) , \tag{13}$$

where $R(s, t_i)$ is the Regge amplitude evaluated on mass shell, A_2 is the contribution from the cuts in the mass variables, and $A_3(s,t)$ is the contribution from the large semicircles. This last term is negligible because of Eq. (12). The first term in Eq. (13) is the usual AFS amplitude [but without the complex conjugation of $R(s, t_2)$ - see Part III).

On the other hand, if we were to close the contour of s_i integration in the upper half plane, we would obtain for $A(s,t)$ only a term similar to $A_3(s,t)$, which vanishes as $s \to \infty$. Hence we conclude that $A(s,t)$ must vanish as $s \to \infty$ (the Feynman parameter technique referred to earlier gives $\ell n\ s/s^3$), and the apparent cut of the first term in Eq. (13) is cancelled by $A_2(s,t)$.

3.   DIAGRAMS WITH CUTS

We now turn to diagrams that do have cuts, leading to the general diagram of Sec. 5 that will connect with our ideas of the composite structure of physical particles and yield the absorption model.

First we consider the double cross diagram of Fig. 8. We briefly review the treatment of Gribov (1968)[18], and then extend the analysis further to obtain a result resembling the absorption model.
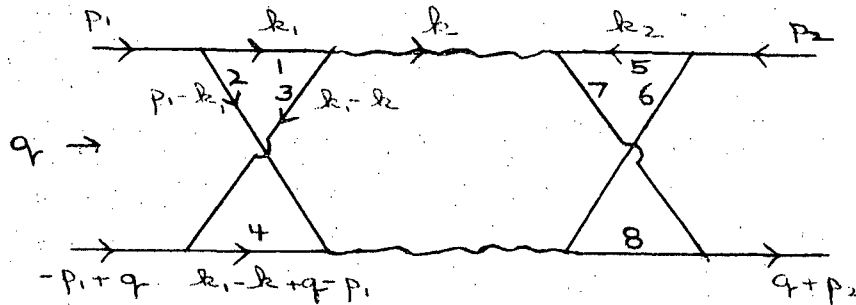
Fig. 8

The amplitude of Fig. 8 is given by[16,18]

$$A(s,t) = i \int \frac{d^4k \, d^4k_1 \, d^4k_2}{\prod\limits_{1}^{8} d_i} R(k_1,k_2,k) \, R'(p_i - k_1, \, p_2 - k_2, \, q - k) \, .$$

$$(14)$$

The essential feature of the analysis is to note from Eq. (12) that the internal Regge amplitudes R and R' become small if their external masses d_i become large as fast or faster than s. Therefore, the dominant contribution to Eq. (14) comes from the region of integration where d_i remains finite relative to s as s goes to infinity.

After s has become asymptotic, the integration over the remaining large values of d_i can be completed. To express this precisely, let Λ be a finite number, and define

$$A_\Lambda(s,t) = i \int d^4k \, d^4k_1 \, d^4k_2 \, R \, R' \prod_1^8 \frac{\Theta(\Lambda - d_i^2)}{d_i} \quad . \tag{15}$$

Then, the above arguments state that the leading behavior of $A(s,t)$ is given by

$$\lim_{s\to\infty} A(s,t) = \lim_{\Lambda\to\infty} \{\lim_{s\to\infty} A_\Lambda(s,t)\} \quad . \tag{16}$$

To perform the analysis embedded in Eq. (15) and Eq. (16), it is convenient to replace the external momenta p_1, p_2 by light-like momenta p_1', p_2' defined by

$$p_1'^2 = p_2'^2 = 0 \, , \qquad 2p_1' \cdot p_2' = s \quad . \tag{17}$$

To order $1/s$ they are given by

$$p_1' = p_1 - \frac{m^2}{s} p_2 \, , \qquad p_2' = p_2 - \frac{m^2}{s} p_1 \quad . \tag{18}$$

The momentum transfer is given by

$$q = \frac{t}{s} (p_2' - p_1') + Q \quad , \tag{19}$$

where Q is a two dimensional vector perpendicular to the incident vectors p_1, p_2.

It is also convenient to introduce new variables of integration (the Sudakov variables) defined by

$$k = \alpha p_2' + \beta p_1' + K \tag{20a}$$

$$k_i = \alpha_i p_2' + \beta_i p_1' + K_i , \qquad i = 1,2 \tag{20b}$$

where K, K_i are again two dimensional vectors perpendicular to p_1, p_2. In terms of these variables, the denominators for the left side of Fig. 8 become

$$d_1 = k_1^2 - m^2 + i\epsilon = \alpha_1 \beta_1 s + K_1^2 - m^2 + i\epsilon \tag{21a}$$

$$d_2 = (p_1 - k_1)^2 - m^2 + i\epsilon = (\alpha_1 - \frac{m^2}{s})(\beta_1 - 1)s + K_1^2 - m^2 + i\epsilon \tag{21b}$$

$$d_3 = (k_1 - k)^2 - m^2 + i\epsilon = (\alpha_1 - \alpha)(\beta_1 - \beta)s + (K_1 - K)^2 - m^2 + i\epsilon \tag{21c}$$

$$d_4 = (k_1 - k + q - p_1)^2 - m^2 + i\epsilon = (\alpha_1 - \alpha + \frac{t}{s} - \frac{m^2}{s})(\beta_1 - \beta - \frac{t}{s} - 1)s$$
$$+ (K_1 - K - Q)^2 - m^2 + i\epsilon \tag{21d}$$

with similar expressions on the right side. The energies of the internal Reggeons become

$$U_1 = (k_1 + k_2)^2 = (\alpha_1 + \alpha_2)(\beta_1 + \beta_2)s + (K_1 + K_2)^2 \tag{22a}$$

$$U_2 = (p_1 + p_2 - k_1 - k_2)^2 = (1 + \frac{m^2}{s} - \alpha_1 - \alpha_2)(1 + \frac{m^2}{s} - \beta_1 - \beta_2)s$$
$$+ (K_1 + K_2)^2 . \tag{22b}$$

And the momentum transfers become

$$k^2 = \alpha\beta s + K^2 \tag{22c}$$

$$(q - k)^2 = (\frac{t}{s} - \alpha)(-\frac{t}{s} - \beta)s + (Q - K)^2 . \tag{22d}$$

The transformation of volume elements is

$$d^4k = \frac{|s|}{2} d\alpha \, d\beta \, dK \text{ , etc.} \tag{22e}$$

The direct channel energies of the left and right crosses are

$$s_1 = (p_1 - k)^2 = (1 - \beta)(\frac{m^2}{s} - \alpha)s + K^2 \tag{22f}$$

$$s_2 = (p_2 + k)^2 = (1 + \alpha)(\frac{m^2}{s} + \beta)s + K^2 . \tag{22g}$$

We can now perform the analysis of Eq. (15) and Eq. (16). We are first to find the region of integration over which $d_i \leq \Lambda$. By solving the equations $d_1, d_2 = 0(\Lambda)$ for α_1, β_1, we find from Eq. (21a,b)

$$\alpha_1 = 0(\frac{\Lambda}{s}) , \qquad \beta_1 = 0(\Lambda) , \tag{23a}$$

while from $d_3, d_4 = 0(\Lambda)$,

$$\alpha = 0(\frac{\Lambda}{s}), \qquad \beta = 0(\Lambda) . \tag{23b}$$

From a similar analysis on d_5, d_6, d_7, d_8 we get

$$\beta, \beta_2 = 0(\frac{\Lambda}{s}) ; \qquad \alpha, \alpha_1 = 0(\Lambda) . \tag{23c}$$

Combining all results, we conclude that the dominant region of integration as $s \to \infty$ is given by

$$\alpha_1, \alpha, \beta, \beta_2 = O(\frac{\Lambda}{s}) \; ; \quad \beta_1, \alpha_2 = O(\Lambda) \; . \tag{24}$$

Comparing Eq. (24) with Eqs. (21), (22), we see that we can neglect β relative to β_1, and α relative to α_2. Changing variables $\alpha_1 s \to \alpha_1$, $\alpha s \to \alpha$, $\beta s \to \beta$, $\beta_2 s \to \beta$, Eq. (21) becomes

$$d_1 = \alpha_1 \beta_1 + K_1^2 - m^2 + i\epsilon \tag{24a}$$

$$d_2 = (\alpha_1 - m^2)(\beta_1 - 1) + K_1^2 - m^2 + i\epsilon \tag{24b}$$

$$d_3 = (\alpha_1 - \alpha)\beta_1 + (K_1 - K)^2 - m^2 + i\epsilon \tag{24c}$$

$$d_4 = (\alpha_1 - \alpha + t - m^2)(\beta_1 - 1) + (K_1 - K - Q)^2 - m^2 + i\epsilon \tag{24d}$$

the Regge energies become

$$U_1 \to \alpha_2 \beta_1 s \tag{25a}$$

$$U_2 \to (1 - \alpha_2)(1 - \beta_1)s \; , \tag{25b}$$

the momentum transfers become

$$k^2 = K^2 \tag{25c}$$

$$(q - k)^2 = (Q - K)^2 \tag{25d}$$

and the direct channel energies are

$$s_1 = m^2 - \alpha + K^2 \qquad\qquad (25e)$$

$$s_2 = m^2 + \beta + K^2 . \qquad\qquad (25f)$$

The factors α_2, β_1, etc. in Eq. (25a,b) tell what fraction of the original energy s flows through the Reggeons and what portion flows down the sides of the diagram. (We shall see later than $0 \le \alpha_2$, $\beta_1 \le 1$.) We see that the terms $d_1, \cdots, d_4$ depend only on the variables of the left loop—α_1, β_1, K_1—and on α, K, but not on β. Similarly for the terms $d_5, \cdots, d_8$.

Next we assume that the Regge amplitudes of Eq. (15) can be written in the factorized form

$$R = g_1(d_1, d_3, k^2) \, e^{-\frac{i\pi}{2}\phi_1(k^2)} U_1^{\phi_1(k^2)} g_2(d_5, d_7, k^2) \qquad (26a)$$

$$R' = g_1'\left(d_2, d_4, (q-k)^2\right) e^{-\frac{i\pi}{2}\phi_2[(q-k)^2]} U_2^{\phi_2[(q-k)^2]} g_2\left(d_6, d_8, (q-k)^2\right) . \qquad (26b)$$

Then, Eq. (15) can be recast into the following form:

$$A_\Lambda(s,t) \propto \int_{0(\Lambda)} dK \left(e^{-\frac{i\pi}{2}}s\right)^{\phi_1(K^2)+\phi_2[(Q-K)^2]-1} N_1(K,Q) N_2(K,Q) \qquad (27a)$$

$$N_1(K,Q) = \int_{0(\Lambda)} d\alpha \, \frac{d\alpha_1 \, d\beta_1 \, dK_1}{\prod_1^4 d_i} \, g_1 g_1' \, \beta_1^{\phi_1} (1-\beta_1)^{\phi_2} \qquad (27b)$$

$$N_2(K,Q) = \int_{0(\Lambda)} d\beta \, \frac{d\alpha_2 \, d\beta_2 \, dK_2}{\prod_5^8 d_i} \, g_2 g_2' \, \alpha_2^{\phi_1} (1-\alpha_2)^{\phi_2} . \qquad (27c)$$

Here we see that A_Λ is an integral over the usual energy term $s^{\phi_1+\phi_2-1}$, times structure functions N_1 and N_2 that involve the Feynman amplitudes, form factors, and the Regge energy factors on each side of the diagram.

To bring Eq. (27) to a more recognizable form, we first let $\Lambda \to \infty$ in accord with Eq. (16). Next, we define the amplitude $A_1(\alpha,K,Q)$ by

$$A_1(\alpha,K,Q) = \int_{-\infty}^{+\infty} \frac{d\alpha_1\, d\beta_1\, dK_1}{\prod_1^4 d_i} \, g_1 g_1' \, \beta_1^{\phi_1}(1-\beta_1)^{\phi_2}. \qquad (28)$$

Note from Eq. (28) that β_1 runs between 0 and +1 only. If $\beta_1 < 0$, then the integrand, as a function of α_1, has singularities that all lie in the upper half plane [see Eq. (24) and Fig. 9]; the α_1 contour of integration can be closed in the lower half plane to give zero. If $\beta_1 > 1$, the singularities all lie in the lower half plane. But if $0 < \beta_1 < 1$, then the singularities pinch the contour of integration and the integral is nonzero.
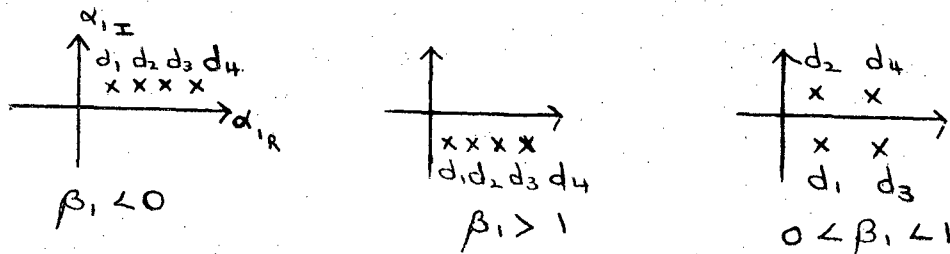

Fig. 9

Next we observe that except for the extra factors in the numerator of Eq. (28), A_1 is the amplitude $\bar{A}_1(s_1,t; t_1,t_2)$ of the Feynman diagram of Fig. 10.
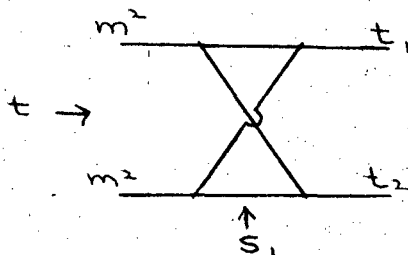
Fig. 10

The form factors g_1, g_1' are functions of the invariants d_i and t_1, t_2. It is easily seen that β_1 is also an invariant of the diagram of Fig. 9. Therefore we can write

$$A_1 = A_1(s_1, t; t_1, t_2) .$$ (29a)

Equation (27) can then be written as

$$A(s,t) \propto \int \frac{dt_1\, dt_2}{(-\lambda)^{\frac{1}{2}}} \left(\frac{s}{\tilde{\imath}}\right)^{\phi_1(t_1)+\phi_2(t_2)-1} N_1(t,t_1,t_2)\, N_2(t,t_1,t_2)$$ (29b)

$$N_i(t,t_1,t_2) = \int_{-\infty}^{+\infty} ds_i\, A_i(s_i,t; t_1,t_2)$$ (29c)

$$A_1(s_i,t; t_1,t_2) = \int_0^1 d\beta_1\, \beta_1^{\phi_1}(1-\beta_1)^{\phi_2} \int_{-\infty}^{+\infty} \frac{d\alpha_1\, dK_1\, q_1 q_1'}{\prod_1^4 d_i}$$ (29d)

with similar expression for A_2.

To bring Eq. (29b) into a form resembling the absorption model, we shall find it necessary to understand the analytic properties of A_1. In the first place, we note that A_1 has all the singularities that the amplitude $\bar{A}_1$ of Fig. 10 has, because these

are determined by the propagators of Eq. (29d). These singularities

consist of normal thresholds at $s_1 = 4m^2 - i\epsilon$ and $u_1 = 4m^2 - i\epsilon$,

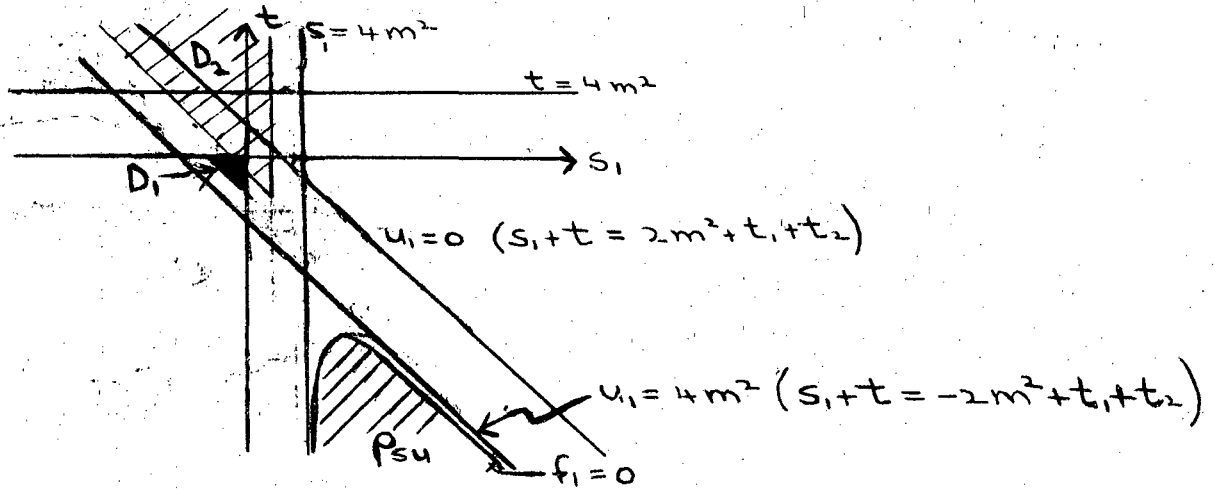and a Landau curve $f_1(s_1, u_1) = 0$ (Fig. 11).

Fig. 11

The singularities introduced in A_1 by the presence of the

form factors g_1, g_1' can be discussed by dispersing in their mass

variables[20,21] and treating the kernels of the transform as propagators.

We have found that they do not change the results below, so for

simplicity we neglect them and take g_1, g_1' as constants.

It remains to discuss the terms $\beta_1^{\phi_1}$, $(1 - \beta_1)^{\phi_2}$. We

assume the trajectories satisfy $\phi_i > -1$, so that these terms by

themselves are integrable. However it is possible that at $\beta_1 = 0,1$

they can pinch with a singularity of the propagators and introduce a

new singularity into A_1. We have been able to investigate this

possibility by two different methods, and we present them both.

First Method

      Looking at Fig. 9 with $0 < \beta_1 < 1$, we see that if we close

the α_1 contour of integration in the lower half plane, we pick up

contributions from the poles in α_1 of the terms d_1, d_3. Writing

$d_i(j)$ as the value of d_i at the pole of d_j, and writing

$D_i(j) = \beta_1 d_i(j)$, we obtain

$$A_1(s_1, t; t_1, t_2)$$

$$\propto \iint dK \int_0^1 d\beta_1 \frac{\beta_1^{\phi_1+1}(1 - \beta_1)^{\phi_2}}{d_3(1)} \left\{ \frac{1}{D_2(1)D_4(1)} - \frac{1}{D_2(3)D_4(3)} \right\} , \tag{28}$$

where

$$d_3(1) = -\alpha\beta_1 + (K_1 - K)^2 - K_1^2 \tag{29a}$$

$$D_2(1) = -[m^2 - \beta_1(1 - \beta_1)(m^2 + \alpha - t)] + (1 - \beta_1)K_1^2 + \beta_1(K_1 + Q - K)^2 \tag{29b}$$

$$D_2(3) = -[m^2 - \beta_1(1 - \beta_1)(m^2 - \alpha)] + \beta_1 K_1^2 + (1 - \beta_1)(K_1 - K)^2 \tag{29c}$$

$$D_4(1) = -[m^2 - \beta_1(1 - \beta_1)(m^2 + \alpha - t)] + (1 - \beta_1)K_1^2 + \beta_1(K_1 + Q - K)^2 \tag{29d}$$

$$D_4(3) = -[m^2 - \beta_1(1 - \beta_1)(m^2 - t)] + \beta_1(K_1 - K + Q)^2 + (1 - \beta_1)(K_1 - K)^2 . \tag{29e}$$

We immediately see that at the endpoints of integration - $\beta_1 = 0,1$ -

the terms $D_i(j)$ are strictly negative and cannot vanish. The term

$d_3(1)$ can vanish, but its residue is zero [i.e., $d_3(1)$ is a factor of the terms in the brackets]. Hence we conclude that the terms $\beta_1^{\phi_1}$, $(1 - \beta_1)^{\phi_2}$ do not introduce any new singularities.

Finally, we observe that A_1 is a real quantity for those values of its arguments for which the $D_i(j)$'s are negative for all β_1 between 0 and 1. This occurs when the terms in brackets of Eq. (29b-e) are positive. Since the maximum value of $\beta_1(1 - \beta_1)$ is $1/4$, this condition is satisfied for

$$4m^2 > m^2 + \alpha - t, \quad m^2 - \alpha, \quad m^2 - t . \tag{30a}$$

This is equivalent to the region

$$s_1 < 4m^2 + K^2, \quad -3m^2 < t < 0, \quad s_1 + t > -2m^2 + K^2 \tag{30b}$$

and is shown in Fig. 11 as region D_1.

Combining this with the earlier result, we conclude:
$A_1(s_1,t; t_1,t_2)$ is real analytic in the same region as
$\bar{A}(s_1,t; t_1,t_2)$, and has the same singularities.

Second Method[25]

Introduce Feynman parameters[20,22] into Eq. (28) via

$$\prod_{j=1}^{4} \frac{1}{d_j} = \left(\frac{1}{i}\right)^4 \int_0^\infty \prod_1^4 d\lambda_j \, e^{i \sum_1^4 \lambda_j d_j} . \tag{31}$$

(The $i\epsilon$ in d guaranties convergence.) Then, the dK_1 integration can be done directly. The $d\alpha_1$ integration can be done using

$$\int_{-\infty}^{+\infty} d\alpha \; e^{i\alpha B} \; \propto \; \delta(B) \; . \tag{32a}$$

The coefficient B involves β_1, and this allows the $d\beta_1$ integral to be performed. We find

$$\beta_1 \; = \; \frac{\lambda_2 + \lambda_4}{\lambda_1 + \lambda_2 + \lambda_3 + \lambda_4} \; , \tag{32b}$$

and

$$A_1(s_1,t; \; t_1,t_2) \; \propto \; \int_0^\infty \prod_1^4 d\lambda_j \left(\frac{\lambda_2 + \lambda_4}{C} \right)^{\phi_1} \left(\frac{\lambda_1 + \lambda_3}{C} \right)^{\phi_2}$$

$$\times \; \frac{e^{iD(\lambda,s_1,u_1)/C(\lambda)}}{[C(\lambda)]^2} \tag{33a}$$

where

$$D(\lambda,s_1,u_1) \; = \; \lambda_2\lambda_3 s_1 + \lambda_1\lambda_4 u_1 + \lambda_1\lambda_3 t_1 + \lambda_2\lambda_4 t_2 + m^2(\lambda_1\lambda_2 + \lambda_3\lambda_4)$$

$$- \; m^2 C(\lambda)^2 \tag{33b}$$

$$C(\lambda) \; = \; \lambda_1 + \lambda_2 + \lambda_3 + \lambda_4 \tag{33c}$$

$$s_1 + t + u_1 \; = \; 2m^2 + t_1 + t_2 \; . \tag{33d}$$

This can be written in the more familiar Feynman representation as

$$A_1(s_1,t; \; t_1,t_2) \; \propto \; \int_0^1 \prod_1^4 d\alpha_i \; \delta(1 - C) \left(\frac{\alpha_2 + \alpha_4}{C} \right)^{\phi_1} \left(\frac{\alpha_1 + \alpha_3}{C} \right)^{\phi_2}$$

$$\times \; \frac{1}{[D(\alpha,s_1,u_1)]^2} \; . \tag{33e}$$

Note that for $\phi_1 = \phi_2 = 0$, A_1 reduces to $\bar{A}_1$.

From Eq. (33) the analytic properties of A_1 can be read off instantly. First, A_1 has the same Landau curves as $\bar{A}_1$, because these come from $D(\alpha, s_1, u_1)$. Second, the term $\beta_1^{\phi_1}$ does not introduce a new singularity, because if $\alpha_2 = \alpha_4 = 0$, then

$$D(\alpha, s_1, u_1) = \alpha_1 \alpha_3 t_1 - (\alpha_1 + \alpha_3)^2 m^2 ; \qquad (34a)$$

since $t_1 < 0$, D is strictly negative and cannot pinch with $\beta_1^{\phi_1}$. Finally, it can be seen from Eq. (33b) that for

$$s_1, u_1 \not\gtrless 2m^2 , \qquad (34b)$$

D is strictly negative. Therefore A_1 is strictly real. This region, labelled D_2, is shown in Fig. 11.

Hence we reach the same conclusions as before. (The region D_2 is larger than D_1, but of course A_1 is real where $\bar{A}_1$ is in both cases because they have the same singularities.)

We summarize the results in Fig. 12a
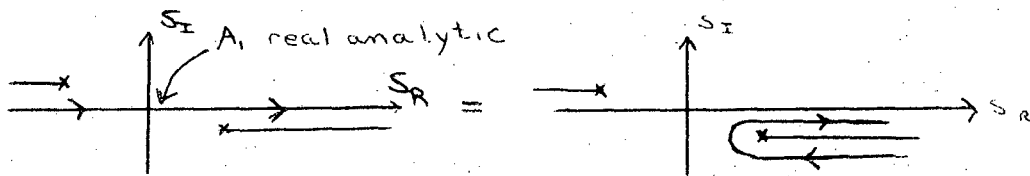
Fig. 12

We can now bring $A(s,t)$ to the form of the absorption model. In Fig. 12 we distort the contour of integration around the right hand

cut. Since $\overline{A}$ behaves as $1/s_1^2$ as $s_1 \to \infty$, therefore so does A_1. (At the endpoints $\alpha_2 \sim \alpha_3 \sim 0$, β_1 and $(1 - \beta_1)$ do not vanish, so A_1 has the same asymptotic behavior as $\overline{A}_1$.) Therefore

$$N_1(t,t_1,t_2) \propto \int_{4m^2}^{\infty} ds_1 \, \text{disc}[A_1(s_1,t; \, t_1,t_2)] \, . \tag{35a}$$

Since A_1 is real analytic between the cuts of Fig. 12a, note that

$$\text{disc}[A_1] = 2i \, \text{Im} \, A_1 \, . \tag{35b}$$

Since the discontinuity is generated by the denominators d_2, d_3, and since A_1 is real analytic, we can invoke a Cutkosky type theorem to give

$$N_1(t,t_1,t_2) \propto i \int_{4m^2}^{\infty} ds_1 \int \frac{d\alpha_1 \, d\beta_1 \, dK_1}{d_1 d_4} \, \beta_1^{\phi_1}(1 - \beta_1)^{\phi_2} \, \delta(d_2)\delta(d_3) F \tag{35c}$$

where F involves the Jacobian of the transformation to mass variables. Integrating on the δ functions

$$N_1(t,t_1,t_2) \propto i \int_{4m^2}^{\infty} ds_1 \int dK_1 \, B^U B^{*L} \tag{35d}$$

where

$$B^U = \frac{\beta_1^{\phi_1}}{d_1} \, (F)^{\frac{1}{2}} \Bigg|_{d_2=d_3=0} \quad , \quad B^L = \frac{(1 - \beta_1)^{\phi_1}}{d_4} \, (F)^{\frac{1}{2}} \Bigg|_{d_2=d_3=0} \, . \tag{35e}$$

In terms of graphs,

$$
N_1 = \int_{-\infty}^{+\infty} ds_1 \; \text{⧓} \quad = \int_{4m^2}^{\infty} ds_1 \; \text{⧓} = i \int_{4m^2}^{\infty} ds_1 \int dK_1 \; \text{⧓}
$$

(35f)

Thus we see that we can split N_1 into an integral of factors $B^U B^L$, where B^U involves the upper part of the diagram, and B^L involves the lower part. Now perform the same operation on N_2,

$$
N_2 \; \propto \; i \int_{4m^2}^{\infty} ds_2 \int dK_2 \; C^U C^{L*} \; .
$$

(35g)

Collecting Eq. (35f,g) and returning to Eq. (29b), we can bring $A(s,t)$ to the form

$$
A(s,t) \; \propto \; \frac{-i}{s} \int \frac{dt_1 dt_2}{(-\lambda)^{\frac{1}{2}}} \, dK_1 \; dK_2 \left\{ B^U (\tfrac{s}{i})^{\phi_1(t_1)} C^U \right\} \left\{ B^{L*} (\tfrac{s}{i})^{\phi_2(t_2)} C^{L*} \right\}
$$

(36a)

Writing

$$
M_1 \; = \; B^U \left(\tfrac{s}{i}\right)^{\phi_1} C^U, \qquad M_2 \; = \; B^L \left(\tfrac{s}{i}\right)^{\phi_2} C^L
$$

(36b)

we finally arrive at

$$
A(s,t) \; \propto \; \frac{-i}{s} \int dK \; dK_1 \; dK_2 \; M_1 \; M_2^* \; e^{-i\pi\phi_2(t_2)}
$$

(36c)

where

$$M_1 = $$

$$M_2 = $$

and

$$A(s,t) \propto -\frac{i}{s} \int d\Omega \quad (\ \ )^* \ e^{-i\pi\phi_2} \tag{36d}$$

$$= -\frac{i}{s} \int d\Omega \tag{36e}$$

We shall extend Eq. (36) to more general diagrams. With B,C real, Eq. (36a) agrees with the absorption model. In particular, when ϕ_1 is the Pomeranchuk, then $A(s,t)$ interferes destructively with the pole term of ϕ_2. For more general B,C, $A(s,t)$ is written in Eq. (36c), with the extra phase term introduced to restore the correct phase to the M_2 amplitude.
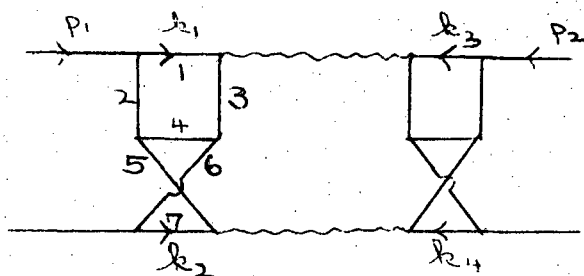
Fig. 13

As an extension of the work above and as preparation for the general diagram of Sec. 5, we briefly discuss the diagram of Fig. 13. There are several noteworthy features.

In the first place, one sees that on the left side of the
diagram only the lines 1,3,5,7 attach to Regge amplitudes. Hence
we might suspect that only these are subject to the finite mass
condition. It turns out this would not give enough conditions to
provide an immediate solution for the Sudakov variables. There are
two ways we can argue to extend the class 1,3,5,7. On the one hand
we can argue that, in the spirit of Arnold, HPKR, and of the work to
follow in Part II, the external physical particles should themselves
also be Reggeized. This would place form factors on the external
vertices also, and would lead to the requirement that the lines 2,6
also satisfy the finite mass condition, and would provide enough
lines to perform the Gribov analysis. On the other hand, Polkinghorne[23]
has recently extended the Gribov analysis to diagrams with internal
Reggeons constructed from Veneziano amplitudes without any form
factors at all. The integrations are done by a steepest descent
analysis, and as it turns out this leads to the desired finite mass
conditions on all internal lines.

In any event, after carrying out the finite mass conditions,
one finds, analogous to before,

$$\alpha_1, \alpha_2, \alpha, \beta, \beta_3, \beta_4 \sim \Lambda/s \tag{36a}$$

$$0 < \beta_1, \beta_2, \alpha_3, \alpha_4 < 1 \quad . \tag{36b}$$

Proceeding as before, one obtains the amplitude $A(s,t)$ in the same
form as before, with the amplitude $A_1(s_1,t; t_1,t_2)$ now given by

$$A(s_1,t; t_1,t_2) = \int_0^1 d\beta_1 \; d\beta_2 \; \beta_1^{\phi_1} \; \beta_2^{\phi_2} \; g_1 g_2 \int_{-\infty}^{+\infty} \frac{d\alpha_1 \, d\alpha_2 \, dK_1 \, dK_2}{\prod_1^7 d_i} \; .$$

(37a)

The amplitude $N_1(t,t_1,t_2)$ is given by a sum of four unitarity terms

$$N = \int_{-\infty}^{+\infty} ds_1 \; \overline{\underline{\bigtimes}} \quad = \int_{4m^2}^{\infty} ds_1 \left\{ \overline{\underline{\bigtimes}}^- + \underline{\bigtimes}_- \right\} + \int_{4m^2}^{\infty} ds_1 \left\{ \bigtimes + \bigtimes \right\}$$

(37b)

Therefore, $A(s,t)$ takes the form

$$A(s,t) \; \propto \; \sum_{i,j} \frac{-i}{s} \int d\Omega_i \, \{ B_i^U \left(\frac{s}{i}\right)^{\phi_1} C_j^U \} \{ B_i^{L*} \left(\frac{s}{i}\right)^{\phi_2} C_j^{L*} \} \; ,$$

(37c)

a sum of all possible unitarity cuts on the left side of the diagram

times all possible cuts on the right.

4. DIAGRAMS WITHOUT CUTS

We now pass on to diagrams that do not have cuts. The essential point we shall demonstrate is that a diagram has a cut if it has third double spectral functions on its sides. As we shall see in Part II, this will tie in conveniently with our physical ideas about the composite structure of physical particles.

The manner in which we shall demonstrate this relation is to show that the amplitude of any diagram with two Reggeon exchange (Fig. 14) can be brought to the form

$$A(s,t) \propto \int dK (\frac{s}{1})^{\phi_1 + \phi_2 - 1} N_1 N_2 \qquad (38a)$$
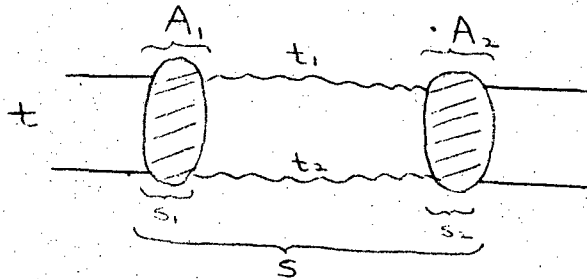
Fig. 14
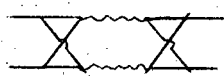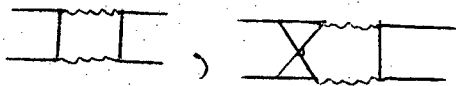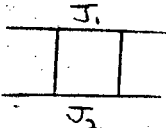
where N_i is related[24] to the amplitude of the blobs

$$N_1(t,t_1,t_2) \sim \int_{-\infty}^{+\infty} ds_1 \, A_1(s_1,t; \, t_1,t_2) \, . \qquad (38b)$$

Furthermore, if A_1 has a third double spectral function, then the integral in Eq. (38b) is nonzero, but if A_1 has no third double spectral function, then N_1 is identically zero. For the second

case, this means that Eq. (38a) is also zero, and that the leading
behavior of $A(s,t)$ is given by a lower order (in s) term than that
of Eq. (38a).

We shall bring our amplitudes, then, to the form of Eq. (38a)
because it focuses so sharply on the requirement of a third double
spectral function. In addition, Eq. (38a) lends itself to a general
definition proposed by F. Henyey that we would like to make. Namely,
we will say that a diagram involving the exchange of two particles of
spin J_1 and J_2 <u>persists</u> if its asymptotic behavior is given by
$s^{J_1+J_2-1}$, to within powers of logarithms. As examples we list:

	leading behavior	persists?
	$s^{\phi_1+\phi_2-1}/\ell n\ s$	yes
	$\sim 1/s^3$	no
	$\ell n\ s \cdot \frac{1}{s}$	yes (spin of is 0)
	$\sim s^{J_1+J_2-1}$	yes

We saw earlier in Sec. 2 that the AFS diagram does not persist
because its leading behavior vanishes as $s \to \infty$ [Eq. (13) and seq.].

We now show quickly that its amplitude can be brought to the form of
Eq. (38a), even though the coefficients N_1, N_2 are zero. To do this,
we apply the Gribov analysis to Fig. 15.
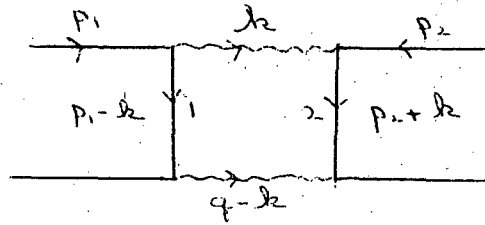
Fig. 15

Then, we have

$$d_1 = (p_1 - k)^2 = (1 - \beta)\left(\frac{m^2}{s} - \alpha\right) s + K^2 - m^2 + i\epsilon$$

$$d_2 = (p_2 + k)^2 = (1 + \alpha)\left(\frac{m^2}{s} + \beta\right) s + K^2 - m^2 + i\epsilon$$

$$t_1 = k^2 = \alpha\beta s + K^2 \tag{39}$$

$$t_2 = (k - q)^2 = \left(\alpha - \frac{t}{s}\right)\left(\beta + \frac{t}{s}\right) s + (K - Q)^2$$

$$U_1 = U_2 = s \ .$$

To satisfy $d_1, d_2 \sim O(\Lambda)$, we obtain

$$\alpha \sim \beta \sim O(\Lambda/s) \tag{40}$$

in which case, with $\alpha \to \alpha s$, $\beta \to \beta s$, we have

$$d_1 = -\alpha + K^2 + i\epsilon$$

$$d_2 = \beta + K^2 - i\epsilon$$

$$t_1 = K^2 \tag{41}$$

$$t_2 = (K - Q)^2 \ .$$

Since we have kept d_1, d_2 finite as s went to infinity, we can write the Regge amplitudes in factorized form

$$R = g_1(d_1, t_1)(\tfrac{s}{i})^{\phi_1(t_1)} g_2(d_2, t_2)$$

$$ \tag{42}$$

$$R' = g_1(d_1, t_1)(\tfrac{s}{i})^{\phi_2(t_2)} g_2(d_2, t_2) .$$

And hence, the amplitude for Fig. 15 takes the form we anticipated all along

$$A(s,t) \propto \int_{-\infty}^{+\infty} dK \cdot \frac{d\alpha\, d\beta}{d_1 d_2} g_1\, g_1' \left(\frac{s}{i}\right)^{\phi_1 + \phi_2 - 1} g_2\, g_2'$$

$$= \int_{-\infty}^{+\infty} dK\, N_1(t, t_1, t_2)\left(\frac{s}{i}\right)^{\phi_1 + \phi_2 - 1} N_2(t, t_1, t_2) \tag{43a}$$

$$N_1(t, t_1, t_2)$$

$$= \int_{-\infty}^{+\infty} d\alpha\, \frac{g_1}{d_1}\, g_1' = \int_{-\infty}^{+\infty} ds_1\, A_1(s_1, t;\, t_1, t_2) \tag{43b}$$

$$A_1(s_1, t;\, t_1, t_2)$$

$$= \frac{g_1(d_1, t_1) g_1'(d_1, t_2)}{d_1} . \tag{43c}$$

In Eq. (43b) the integrand, as a function of α, has pole and cut singularities in the lower half plane (Fig. 16). Further, the form
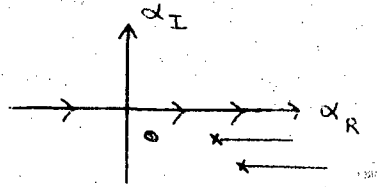
Fig. 17

factors decrease as $d_1 \to \infty$.

$$g_1(d_1, t_1) \to 0 \quad \text{as} \quad d_1 \to \infty$$

Therefore, we can close the α contour of integration in the upper
half plane and get for N_1 zero, as expected. We conclude that Eq.
(38) holds for the AFS amplitude, but its value is zero.

In the discussion of the AFS diagram, we need to invoke
properties of the form factors in order to prove that the amplitude
does not persist. As it turns out, for the diagram of Fig. 18 we
must also employ knowledge of the form factors. However, for diagrams
more complicated (Fig. 20 for example), the absence of the cut rests
completely on the absence of the third double spectral functions.

Consider, Fig. 18.
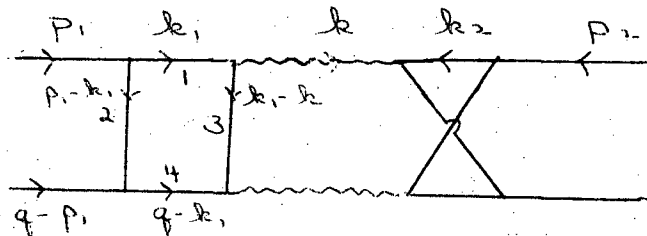
Fig. 18

Applying the finite mass conditions on the right cross we obtain

$$\beta_2, \beta \sim \Lambda/s \; ; \qquad \alpha_2, \alpha \sim \Lambda \tag{44a}$$

and from the left cross

$$\alpha_1, \alpha \sim \Lambda/s; \qquad \beta_1 \sim \Lambda . \tag{44b}$$

The Regge energies become

$$U_1 = (k_1 + k_2)^2 \to \alpha_2 \beta_1 s \tag{45a}$$

$$U_2 = (p_2 + k_1 - k - k_2)^2 \to (1 - \alpha_2) \beta_1 s \tag{45b}$$

and setting $\alpha s \to \alpha$, $\beta s \to \beta$, etc., the denominators on the left become

$$d_1 = \alpha_1 \beta_1 + K_1^2 - m^2 + i\epsilon$$

$$d_2 = (\alpha_1 - m^2)(\beta_1 - 1) + K_1^2 - m^2 + i\epsilon$$

$$\tag{46}$$

$$d_3 = (\alpha_1 - \alpha)\beta_1 + (K_1 - K)^2 - m^2 + i\epsilon$$

$$d_4 = (\alpha_1 - t)\beta_1 + (K_1 - Q)^2 - m^2 + i\epsilon .$$

The amplitude takes the form of Eq. (43a), where now

$$N_1 = \int_{-\infty}^{+\infty} d\alpha \, A_1(\alpha, t; \, t_1, t_2) = \int_{-\infty}^{+\infty} ds_1 \, A_1 \tag{47a}$$

$$A_1 = \int_0^1 d\beta_1 \int_{-\infty}^{+\infty} \frac{d\alpha_1 dK_1}{d_1 d_2 d_3 d_4} \, \beta_1^{\phi_1 + \phi_2} \, g_1(d_1, d_3, t_1) g_1'(d_3, d_4, t_2) \tag{47b}$$

Now as a function of s_1, A_1 has only a right hand cut in the lower half plane, so in Eq. (47b) we are tempted to close the s_1 contour of integration in the upper half plane (Fig. 19).
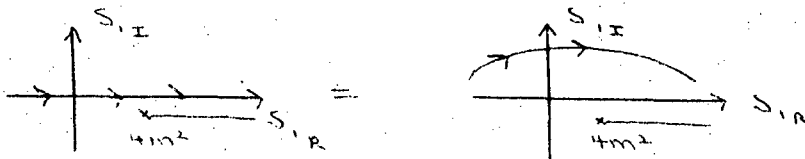
Fig. 19

However, this will not do because for large s_1,

$$A_1(s_1,t;\ t_1,t_2)\ \rightarrow\ \ell n\ s_1/s_1\ .\tag{48}$$

Therefore, the contour cannot necessarily be closed.

We can circumvent this difficulty by interchanging the orders of integration in Eq. (47b,c) and first integration on α. Then

$$N_1\ =\ \int \frac{d\beta_1 d\alpha_1 dK_1}{d_1 d_2 d_4}\ \beta_1^{\not{\phi}_1+\not{\phi}_2}\ \int_{-\infty}^{+\infty} \frac{d\alpha\ q_1 q_2}{d_3}\ .\tag{49}$$

The α-integrand has singularities in α in the upper half plane. The contour can be closed in the lower half plane. Invoking the decrease of g_1, g_2 as d_3 becomes large, we see that the α-integral is zero. The remaining integrals in Eq. (49) converge, and hence $N_1 = 0$.

Finally, we discuss the diagram of Fig. 20, which will lead to the general case of Sec. 5.
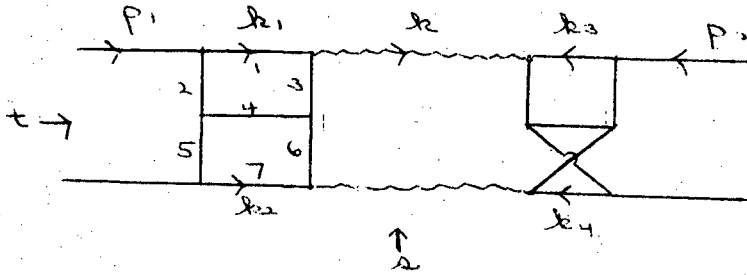
Fig. 20

From the finite mass condition, we obtain

$$\alpha_1, \alpha_2, \alpha, \beta, \beta_3, \beta_4 \sim \Lambda/s$$

$$0 < \beta_1, \beta_2, \alpha_3, \alpha_4 < 1 ,$$

(50)

and this leads to

$$N_1 = \int_{-\infty}^{+\infty} ds_1 \, A_1(s_1, t; \, t_1, t_2)$$

(51a)

$$A_1 = \int \frac{d\alpha_1 \, D\beta_1 \, dK_1 \, d\alpha_2 d\beta_2 dK_2}{\prod_{1}^{7} d_i} \beta_1^{\phi_1} \beta_2^{\phi_2} g_1 g_1' .$$

(51b)

Again, A_1 has only a right cut, but now
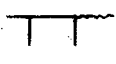
$$A_1 \rightarrow \ell n \, s_1/s_1^2 \qquad \text{as} \quad s_1 \rightarrow \infty$$

and hence the contour of integration in Eq. (51a) can be closed in the upper half plane to give $N_1 = 0$. For Fig. 20 the absence of the cut is thrown entirely on the absence of the third double spectral function.

5.   THE GENERAL CASE

We now come to a general class of two Reggeon exchange diagrams which is the basis for our derivation of the absorption model.   Just how general can this class be?   As we have pointed out before, what we are interested in is the amplitude for a diagram of the type of Fig. 14. However, we do not wish the amplitudes A_i to be completely arbitrary, because in the form of the absorption model we are interested in we require that they be strictly low-energy amplitudes relative to s. That is, we require that the incident energy s flow across the Reggeons and not down the sides of the diagram.   This is because we will want to identify the A_i with direct channel physical particles near mass shell.

Note that the diagrams we have studied satisfy this condition. For example, we have found that while the 4-momenta on the sides of the diagrams can become large   (e.g., $k_1 = \beta_1 p_1' + \alpha_1 p_2' + K_1$, $0 < \beta_1 < 1$, $\alpha_1 \sim \frac{\Lambda}{s}$) the energies s_i remain finite relative to s (e.g., $s_1 = -\alpha s + m^2 + K^2$, $\alpha \sim \Lambda/s$). The large energy s flows only across the Reggeons.

It is not hard to convince oneself that a general type of diagram satisfying these conditions is that of Fig. 21 below.   The effect of the elementary lines $\top \top$ is to tell us where the internal Reggeon line ends and to prevent A_1 from having Regge behavior in s.
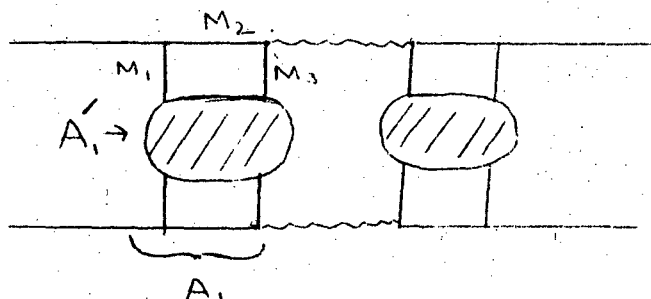
Fig. 21

Thus, Fig. 21 excludes all the diagrams of Fig. 22.
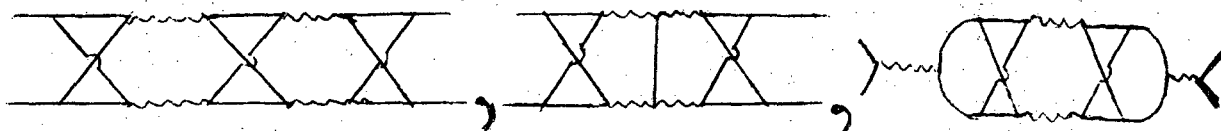
Fig. 22

It includes all the diagrams discussed before. (For the double cross

diagram, A_1' would be various δ-functions.) It also includes the

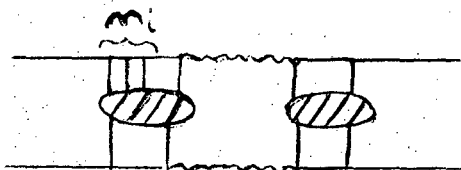diagram of Fig. 23, if the lines n_i are grouped into the mass M_1.

Fig. 23

Most important, it includes the diagram of Fig. 24a. When the rungs

in the direct channel are summed over, this provides a model for the

Regge box diagram of Fig. 24b (first introduced by Arnold and discussed

in HPKR).
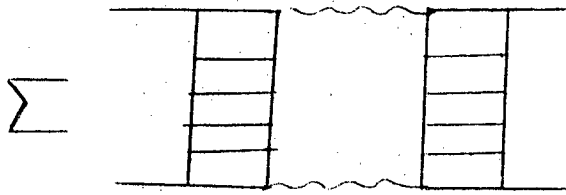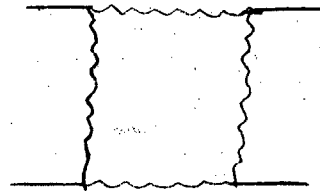
Fig. 24a   Fig. 24b

We consider, then, the diagram of Fig. 25.
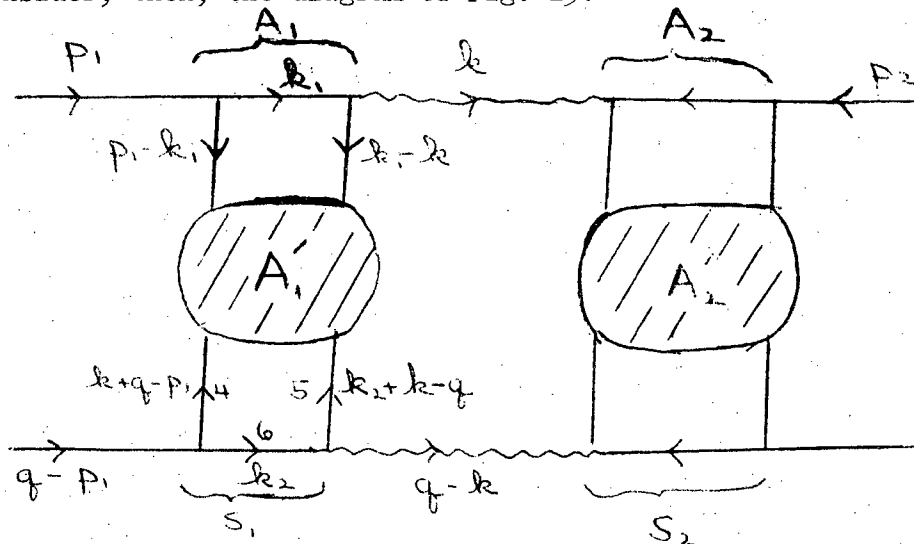
Fig. 25

We use the notation:

$$A = A(s,t)$$

$$A_1 = A_1(s_1,t; t_1,t_2)$$

$$A_1' = A_1(s_1,t_1',u_1'; d_i) .$$

(52)

The amplitude A_1' is to be quite general; we are interested only in whether or not it has a third double spectral function, and so write it in the form

$$A_1' = \int_{4m^2}^{\infty} d\zeta \, \frac{f(s_1,\zeta)}{\zeta - t_1'} + \int_{4m^2}^{\infty} d\zeta \, \frac{g(s_1,\zeta)}{\zeta - u_1'} \quad . \tag{53}$$

That is, we can treat A_1' as a propagator of mass $\zeta \geq 4m^2$. The analysis now goes through as before. We indicate the essential features.

After performing the finite mass analysis, $A(s,t)$ takes the expected form

$$A(s,t) \propto \int dK \left(\frac{s}{1}\right)^{\phi_1 + \phi_2 - 1} N_1 N_2 \tag{54a}$$

$$N_1(t,t_1,t_2) = \int_{-\infty}^{+\infty} ds_1 \, A_1(s_1,t; \, t_1,t_2) \tag{54b}$$

$$A_1(s_1,t; \, t_1,t_2) = \int_0^1 d\beta_1 d\beta_2 \int_{-\infty}^{\infty} \frac{d\alpha_1 d\alpha_2 dK_1 dK_2}{\prod_1^5 d_i} \beta_1^{\phi_1} \beta_2^{\phi_2} g_1 g_2 A_1' \tag{54c}$$

where

$$d_1 = \alpha_1 \beta_1 + K_1^2 - m^2 + i\epsilon$$

$$d_2 = (\alpha_1 - m^2)(\beta_1 - 1) + K_1^2 - m^2 + i\epsilon$$

$$d_3 = (\alpha_1 - \alpha)\beta_1 + (K_1 - K)^2 - m^2 + i\epsilon \tag{55}$$

$$d_4 = \alpha_2 \beta_2 + K_2^2 - m^2 + i\epsilon$$

$$d_5 = (\alpha_2 + t - m^2)(\beta_2 - 1) + (Q + K_2)^2 - m^2 + i\epsilon$$

$$d_6 = (\alpha_2 + t - \alpha)\beta_2 + (K_2 + Q - K)^2 - m^2 + i\epsilon$$

$$s_1 = -\alpha + K^2 + m^2$$

$$u_1 = m^2 + \alpha - t + (K - Q)^2 \tag{56}$$

$$t_1' = (\alpha_2 + t - \alpha_1)(\beta_2 - \beta_1) + (K_2 + Q - K_1)^2 \tag{57}$$

$$u_1' = (\alpha_1 + \alpha_2 + t - \alpha - m^2)(\beta_1 + \beta_2 - 1) + (K_1 + K_2 + Q - K)^2 \quad .$$

We consider separately the cases of the t_1' and u_1' dispersion contributions.

The u_1' Contribution

As before, the first task is to establish the analytic properties of the amplitude A_1. This can again be done either by direct integration on α_1, α_2 or by introduction of Feynman parameters. We briefly discuss each.

Integration on α_1, α_2

Let U denote the denominator $\zeta - u_1'$ in Eq. (53), and consider the integral in Eq. (54c),

$$I = \int\limits_0^1\!\!\int d\beta_1 \, d\beta_2 \int\limits_{-\infty}^{+\infty}\!\!\int \frac{d\alpha_1 \, d\alpha_2}{d_1 d_2 d_3 d_4 d_5 d_6 U} \quad . \tag{58}$$
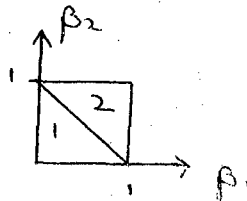
Fig. 26

For $0 < \beta_1 + \beta_2 < 1$, the singularities in α_1, α_2 lie as shown in

Fig. 27a, and for $1 < \beta_1 + \beta_2$ they lie as shown in Fig. 27b.
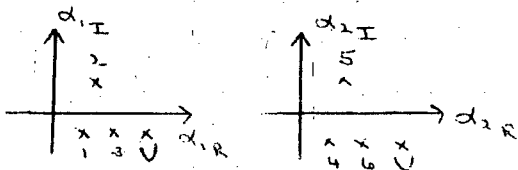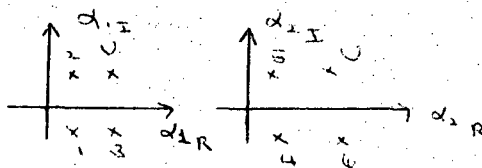

    Fig. 27a   Fig. 27b

Hence in region 1 we close both contours of integration in the upper

half plane, and obtain

$$ I_1 \;=\; \iint\limits_{I} \frac{d\beta_1 d\beta_2\; \beta_1^{\phi_1} \beta_2^{\phi_2}\, (1 - \beta_1)^2\, (1 - \beta_2)^2}{u(2,5)\; D_1(2) D_3(2)\; D_4(5)\quad D_6(5)} \quad . \tag{59} $$

We spare the reader the expressions for $u(2,5)$ and $D_i(j)$, and

simply remark that they have the following properties:

(1) They are strictly negative at $\beta_1, \beta_2 = 0,1$. Therefore the

contribution to I_1 from the endpoints is analytic, and hence

I_1 has no new singularities from the factors $\beta_i^{\phi_i}$.

(2) They are strictly negative for $0 < \beta_1, \beta_2 < 1$ when

$$ s_1 < 4m^2 + k_2^{\,2}, \quad -3m^2 < t < 0 \tag{60} $$

Therefore I_1 is real there.

A similar analysis is carried out for the region 2, this time

closing the α_i contours of integration in the lower half planes

(see Fig. 27b). There are now four contributions of the type of

Eq. (59).

The end result of the analysis is that A_1 has the same real

analytic properties of the amplitude $\overline{A}_1$ defined without the g_i

$\beta_i^{\phi_i}$ terms.

Feynman Parameters[25]

Introducing Feynman parameters as before, the amplitude A_1 takes the form:

$$A_1(s,u_1; t_1,t_2) = \int_{4m^2}^{\infty} d\zeta \, f(s_1,\zeta) \, F_1(s_1,u_1; t_1,t_2,\zeta) \tag{61a}$$

$$F = \int_0^{\infty} d\lambda_1 \cdots d\lambda_7 \, [\beta_1(\lambda)]^{\phi_1} \, [\beta_2(\lambda)]^{\phi_2}$$

$$\chi \; \frac{e^{iD(\lambda,s_1,u_1,\zeta)/C(\lambda)}}{[C(\lambda)]^2} \tag{61b}$$

$$\propto \int_0^1 d\alpha_1 \cdots d\alpha_7 \, \delta(1 - \Sigma\alpha_i) \, \frac{C(\alpha)}{[D(\alpha,s_1,u_1,\zeta)]^3}$$

$$\chi \; [\beta_1(\alpha)]^{\phi_1} \, [\beta_2(\alpha)]^{\phi_2} \tag{61c}$$

where

$$\beta_1(\alpha) = \frac{\alpha_2(\alpha_4 + \alpha_5 + \alpha_6 + \alpha_7) + \alpha_7(\alpha_4 + \alpha_6)}{C(\alpha)} \tag{61d}$$

$$\beta_2(\alpha) = \frac{\alpha_5(\alpha_1 + \alpha_2 + \alpha_3 + \alpha_7) + \alpha_7(\alpha_1 + \alpha_3)}{C(\alpha)} \tag{61e}$$

$$C(\alpha) = \sum_1^7 \alpha_i \tag{61f}$$

$$D = s_1[\alpha_2\alpha_3(\alpha_4 + \alpha_5 + \alpha_6 + \alpha_7) + \alpha_5\alpha_6(\alpha_1 + \alpha_2 + \alpha_3 + \alpha_7) + \alpha_2\alpha_5\alpha_7 + \alpha_3\alpha_6\alpha_7]$$

$$+ u_1 \, \alpha_1\alpha_4\alpha_7$$

$$+ m^2[\alpha_1\alpha_2(\alpha_4 + \alpha_5 + \alpha_6 + \alpha_7) + \alpha_1\alpha_6\alpha_7]$$

$$+ m^2[\alpha_4\alpha_5(\alpha_1 + \alpha_2 + \alpha_3 + \alpha_7) + \alpha_3\alpha_4\alpha_7]$$

$$+ K^2[\alpha_1\alpha_3(\alpha_4 + \alpha_5 + \alpha_6 + \alpha_7) + \alpha_1\alpha_5\alpha_7]$$

$$+ (Q - K)^2[\alpha_4\alpha_6(\alpha_1 + \alpha_2 + \alpha_3 + \alpha_7) + \alpha_3\alpha_4\alpha_7]$$

$$- [\alpha_7\zeta + \sum_1^6 \alpha_i \cdot m^2]$$

$$\times \ [(\alpha_1 + \alpha_2 + \alpha_3)(\alpha_4 + \alpha_5 + \alpha_6) + \alpha_7(\alpha_1 + \alpha_2 + \alpha_3 + \alpha_4 + \alpha_5 + \alpha_6)] \ .$$

$$(61g)$$

The analytic properties of A_1 now follow easily. First, A_1 has all the singularities that $\bar{A}_1$ has, because they are determined by the Feynman discriminate D of Eq. (61g). Second, A_1 does not have any new singularity arising from the β_i factors. If β_1 vanishes, say, then various α_j in Eq. (61d) also vanish. Further, since we have assumed $\phi_1 > -1$, then $\beta_1^{\phi_1}$ is integrable; therefore, we are only interested in those singularities in which the propagators $d_1, \cdots, d_6$ participate. This means that all the remaining α_j's must either vanish or pinch. However, these are just the conditions for a Landau singularity of the Feynman amplitude $\bar{A}_1$. So we can conclude that any singularity of A_1 associated with the vanishing of β_1 must already be a singularity of $\bar{A}_1$. Since the sheet structure of the

singularities is determined by the $i\epsilon$ prescription in D, and is

unaffected by the presence of the $\beta_1^{\emptyset_1}$, we see that A_1 has no more

singularities than $\bar{A}_1$.

Third, it is easily seen from Eq. (61g) that D is strictly

negative for $s_1, u_1 < 2m^2$; hence A_1 is real there.

So we conclude that A_1 has the same real analytic properties

as $\bar{A}_1$.

Now we can return to N_1 [in Eq. (54b)] and bring it to the

unitarity form. Since A_1 has left and right thresholds (Fig. 28),
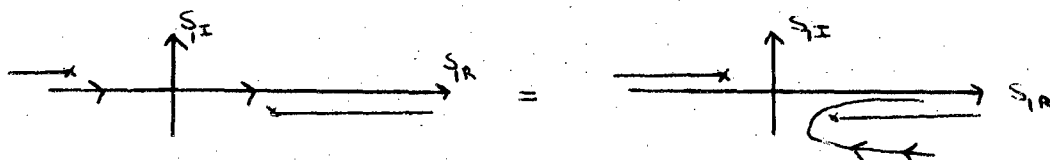
Fig. 28

we can close the contour of integration around the right cut to

obtain

$$N_1 = \sum_i \int_{\triangle_i}^{\infty} ds_1 \ \mathrm{disc}[A_1] = 2i \sum_i \int_{\triangle_i}^{\infty} ds_1 \ B_i^U B_i^{L*} \qquad (62a)$$

$$= \int_{4m^2}^{\infty} ds_1 \left\{ \overline{\square} + \underline{\square} \right\} + \sum_j \int_{\triangle_j}^{\infty} ds_1 \left\{ \overline{\square} + \overline{\square} + \overline{\square} \right\} \qquad (62b)$$

The sums in Eq. (62) are over all possible s_1 channel unitarity cuts.

Returning to Eq. (54a), we again obtain

$$A(s,t) = -2i \sum_{i,j} \int dK \, ds_1 ds_2 \left\{ B_i^U \left(\frac{s}{i}\right)^{\phi_1} C_i^U \right\} \left\{ B_i^{L*} \left(\frac{s}{i}\right)^{\phi_2} C_i^{L*} \right\}. \tag{63}$$

The t_1' Contribution

The calculations proceed as before. One again verifies that A_1 has the same real analytic structure as $\bar{A}_1$. When we come to consider N_1, we observe that as a function of α $(s_1 = -\alpha + K^2 + m^2)$, the integrand of Eq. (54b) has singularities in α from d_3, d_6, s_1 that all lie in the upper half plane. (This is another way of saying that A_1' has no left cut.) Hence we can close the s_1 contour of integration in the upper half plane to get zero. Therefore $N_1 \equiv 0$, and $A(s,t)$ does not persist.

PART II. PHYSICAL IMPLICATIONS, COMPOSITENESS,

MULTIPLE SCATTERING, AND THE ABSORPTION MODEL

Now consider the relationship between the mathematical results
obtained and the physical meaning of compositeness and multiple
scattering. It is not hard to see why the AFS diagram does not give
the double scattering we would expect. On the one hand, the form of
a Reggeon amplitude,

$$t \rightarrow \qquad = g_1(M_1^2, M_2^2, t) \; s^{\phi(t)} \; g_2(M_3^2, M_4^2, t) \quad (64)$$

implies a compositeness of the external particles M_i which is
reflected in the form factor dependence on M_i. It was through just
this dependence that the Rothe cancellation occurs. This compositeness
is also reflected through the ladder representation of a Reggeon,

$$= I + II + III + \cdots . \qquad\qquad (65)$$

On the other hand, when the Reggeon of Eq. (64) is inserted in an
AFS diagram, the external particles M_1, M_4 are given elementary
particle propagators. We claim it is this inconsistency that deprives
the AFS diagram of a cut.

What must be done is either to remove the M_i dependence
from Eq. (64), or to represent the external particles M_i by more
realistic propagators. We would like to discuss the second alternative.

It is our belief, in the spirit of Arnold and HPKR, that physical particles are complicated composite objects. In a Bethe-Salpeter framework, for example, one writes

$$\sum \ \boxed{\ \ \ } \ = \ \bigvee \ + \cdots\cdots\ ,$$

(65)

where the right side represents the physical pole of the left side.

In a scattering process of a physical particle, some of the constituent pieces of matter take part in the scattering, while the rest stands by as a spectator not taking part. A single scattering process that is drawn as
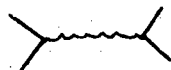
microscopically looks like
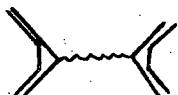
where the double lines are the physical particles and the single lines are their constituents. Similarly, a double scattering process that is drawn as
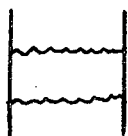
should actually be drawn as
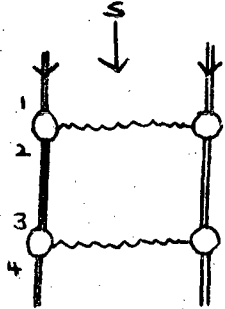
Fig. 29

The incident particle at (1) separates into scattering and spectator

constituents.   At (2) the constituents unite to form a physical

particle in the intermediate state.   At (3) the same process

occurs again, and the physical particle emerges at (4) .

     In a field theory model, the intermediate physical particle

can be represented by the direct channel ladders of Eq. (65).   We

can interpret this as a direct channel Reggeon.   This suggests Fig. 30.
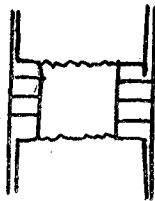
Fig. 30

From the results of Sec. 5, we know Fig. 30 does not have a cut

because the sides lack third double spectral functions. Physically,

this corresponds to an apparent cancellation between the contributions

to $\int ds_1 \, A_1(s_1, t; \, t_1, t_2)$ that come from even and odd signature

physical particles.   A direct channel Reggeon with signature is

represented as
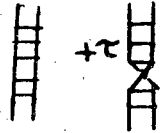
Figure 30 becomes replaced by Fig. 31, which has a cut.
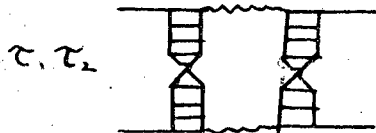
Fig. 31

In a phenomenological calculation, we replace the direct

channel amplitudes of Fig. 31 by the known physical particles. Thus,

for $\pi^- p \to \pi^0 n$,
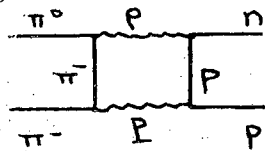
the contribution $\displaystyle\int_{4m^2}^{\infty} ds_2$ disc $A_2(s_2;t; t_1,t_2)$ is written as

Fig. 32

where we include all recurrences of the p and continuum states.

A typical term contributes

$$\int ds_1 \; \text{disc} \left\{ \frac{g_{\rho pn} \; g_{pp\mathbb{P}}}{s_2^2 - mp^2 + i\epsilon} \right\} \propto i \; g_{\rho pn} \; g_{pp\mathbb{P}} \quad .$$

The scattering amplitude becomes

$$A(s,t) \propto -\frac{i}{s} \int dK \, g_{\pi\pi\rho} \left(\frac{s}{1}\right)^{\phi_1} g_{n\rho p} \cdot g_{\pi\pi P}\left(\frac{s}{1}\right)^{\phi_2} g_{ppP} \tag{67a}$$

$$\propto -\frac{i}{s} \int \frac{dt_1 dt_2}{(-\lambda)^{\frac{1}{2}}} \, M_\rho(s,t_1) \, M_{e\ell}(s,t_2) \quad . \tag{67b}$$

This is the absorption model.[33]

In HPKR the contributions of the remaining terms of Fig. 32 are assumed to have the same s,t dependence as that of Eq. (67b), and are added by multiplying Eq. (67b) by a factor λ. It has been shown[26] that the amplitude for

$$p + p \to p + \text{anything} \tag{68a}$$

proceeding via Pomeranchuk exchange, can be as large as 50% of the elastic amplitude

$$p + p \to p + p \ . \tag{68b}$$

This suggests that λ could be about 2.

PART III.   COMPARISON WITH THE WORK OF GRIBOV ET AL

In Ref. 27, Gribov and Migdal studied amplitudes generated

by the exchange of a Regge pole. Their program is to write a Reggeon

field theory that can be solved by summing Reggeon diagrams to determine

the scattering amplitude. For example, the amplitude involving the

Pomeranchuk and the PP cut is given by

Fig. 33

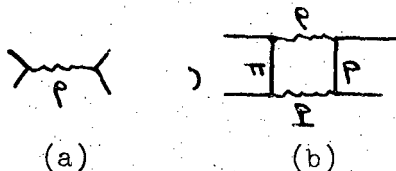This implies for the absorption model that in addition to the diagrams

(a)   (b)
Fig. 34

one must consider effects of t-channel iterations

(a)   (b)   (c)
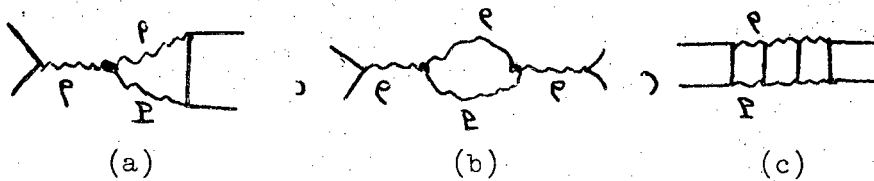
Fig. 35

It is well known that if the diagrams of Fig. 35c are summed, the

sum has a pole term related to the pole of Fig. 34a, and a cut term

related to the cut of Fig. 34b. Is one double counting by including

the pole of Fig. 34a separately? Compelling physical arguments have

been given in HPKR for why this is not so, and that the physics of

elastic absorption is different from the physics of quantum number

exchange.

Gribov et al[27,28] derived the absorption model from diagrams.

We compare their derivation with ours. For their discussion of N_1,

$$N_1 = \int_{-\infty}^{\infty} ds_1 \, A_1(s_1,t; \, t_1,t_2)$$

they write that generally
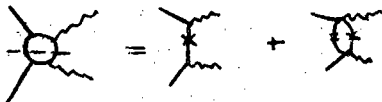
They argue in a general fashion that A_1 has no new singularities or

complexity from the presence of the $\beta_i^{\phi_i}$. Therefore the discontinuity

of A_1 can be calculated as for ordinary amplitudes by cutting the

diagram and replacing the lower amplitude by its complex conjugate.

They also give a proof for elastic scattering that $\lambda > 1$.

Our approach differs from theirs in that we have attempted to

present a specific model for the two Reggeon diagram that is based

on our physical understanding of compositeness and multiple scattering,

and to derive the absorption formula from that model.

Ter-Martirosyan[29] has derived the two Reggeon cut from the
AFS diagram by using form factors for the internal Reggeons that are
evaluated on mass shell. The Rothe cancellation mechanism is removed
and the contribution from the "elementary" propagators evaluated near
mass shell gives the expected form of the cut.

He also considers higher order cuts,
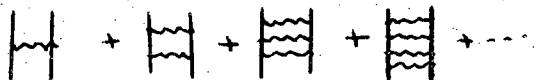
and derives the eikonal formula of Arnold. How do his results affect
ours? In our program we only need to consider the ρP cut. All
elastic multiple scatterings are grouped into a single P term, which
is parameterized and fit by experiment (Fig. a,b).
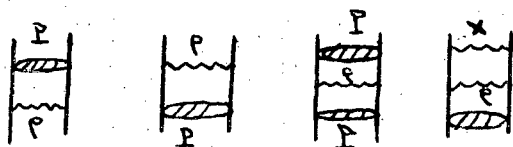
The $PP\rho$ cut (Fig. c) is found to be small. Any cut involving $P\rho$
and a non-Pomeranchon is small because the branch point is well below
the ρ pole.

PART IV. ASSUMPTIONS, CONCLUSIONS, AND FUTURE AREAS OF WORK

Assumptions

1. Physical particles are composite objects and when regarded as Reggeons they have definite signature.

2. Multiple scattering of composite systems can be treated in a Glauber scatterer-spectator approach.

3. The leading behavior of a Feynman amplitude is given by the Gribov-Polkinghorne finite mass conditions; the second order term in this analysis is down by a factor of $1/s$ from the leading behavior.

Conclusions

The amplitude for the diagram
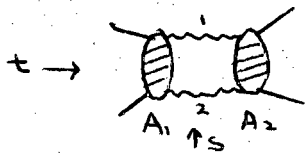
where A_i are low energy amplitudes relative to s, is given by the absorption formula

$$A(s,t) \propto +i \int dK \; s^{\phi_1 + \phi_2 - 1} \; e^{-\frac{i\pi}{2}(\phi_1 + \phi_2)} \; N_1 N_2$$

$$\propto -i \int \frac{dK}{s} \; M_1(s,t_1) \; M_2(s,t_2) + \cdots$$

Future Areas of Work

1. What is the effect of t-channel iterations?

2. What is the relation between the absorption model approach and the bootstrap approach?

3. Is $\lambda > 1$?

ACKNOWLEDGMENTS

REFERENCES

1. T. Regge, Nuovo Cimento 14, 951 (1959).

2. G. E. Hite, Rev. Mod. Phys. 41, 669 (1969).

3. R. J. Eden, P. V. Landshoff, D. I. Olive, and J. C. Polkinghorne,
    The Analytic S-Matrix (Cambridge University Press, 1966).

4. R. J. Eden, High Energy Collisions of Elementary Particles
    (Cambridge University Press, 1967).

5. B. M. Udgaonkar and M. Gell-Mann, Phys. Rev. Letters 8, 346 (1962).

6. E. S. Abers, H. Burkhardt, V. L. Teplitz, and C. Wilkin, Nuovo
    Cimento 42, 365 (1965).

7. F. Henyey, G. L. Kane, and J. Pumplin, Phys. Rev. 182, 1579
    (1969).

8. R. J. Glauber in Lectures in Theoretical Physics (Wiley-Interscience,
    Inc., New York, 1959), Vol. 1.

9. V. Franco and R. J. Glauber, Phys. Rev. 142, 1195 (1966).

10. R. C. Arnold, Phys. Rev. 153, 1523 (1967); Argonne National
    Laboratory Report No. ANL/HEP 6804, 1968 (unpublished).

11. C. B. Chiu and J. Finkelstein, Nuovo Cimento 57A, 649 (1968).

12. D. Amati, S. Fubini, and A. Stanghellini, Phys. Letters 1, 29
    (1962).

13. J. C. Polkinghorne, Phys. Letters 4, 24 (1963).

14. S. Mandelstam, Nuovo Cimento 30, 1127 (1963); 30, 1148 (1963).

15. P. G. Federbush and M. T. Grisaru, Ann. Phys. 22, 263, 299 (1963).

16. H. J. Rothe, Phys. Rev. 159, 1471 (1967).

17. C. Wilkin, Nuovo Cimento 31, 377 (1964).

18. V. N. Gribov, Proceedings of 1967 International Conference on
    Particles and Fields (Wiley-Interscience Inc., New York 1967);
    Sov. Phys.-JETP 53, 654 (1967); Sov. Phys.-JETP 26, 414 (1968);
    V. V. Sudakov, Sov. Phys.-JETP 30, 87 (1956); Sov. Phys.-JETP
    3, 65 (1956).

19. This is also easily seen from a d-line analysis of the Reggeon
    in the ladder representation.

20. I. T. Drummond, P. V. Landshoff, and W. J. Zakrzewski, Nucl. Phys.
    B11, 383 (1969).

21. G. A. Winbow, Cambridge Preprint 68/26.

22. P. V. Landshoff and J. C. Polkinghorne, Cambridge Preprint 68/29.

23. J. C. Polkinghorne, Cambridge Preprint 69/31.

24. J. C. Polkinghorne, Nucl. Phys. B6, 441 (1968).

25. I am very indebted to P. V. Landshoff for suggesting this approach.
    It is much quicker and more elegant than the first method.

26. J. Pumplin and M. Ross, Phys. Rev. Letters 21, 1778 (1968).

27. V. N. Gribov and A. A. Migdal, Yad. Fiz. 8, 1002, 1213 (1968),
    English translation Soviet Journal of Nuclear Physics 8, 583,
    703 (1969).

28. A. B. Kaidalov and B. M. Karnakov, Phys. Letters 29B, 372 (1969).

29. K. A. ter-Martirosyan, I. T. E. P. preprints, summer 1969.

30. A solution to this difficulty, different from the one we present,
    has been suggested by Dr. C. Wilkin, Graphs and Glauber, University
    College Preprints.

31. Where $A_{\pi p} \sim i \, s^{\alpha(t)}$.

32. Where $A_{e\ell} \sim -i \qquad (\alpha(t) \equiv +1)$.

33. Where $M_{e\ell} \sim (\frac{s}{i})^{\alpha(t)}$.